

ACRYLONITRILE BUTADIENE RUBBER/PHENOLIC RESIN BLENDED ABLATIVE COMPOSITES FOR HIGH TEMPERATURE APPLICATIONS

**Nadeem Iqbal¹, Sadia Sagar Iqbal², Abdul Waheed Anwar³,
Afsheen Sarwar⁴, Faiza Jabeen⁵, Sarwat Jabeen⁶**

^{1,4,5,6} Department of Polymer Engineering and Technology, CEET, University of the Punjab, Lahore, (Pakistan),

²School of Chemical & Materials Engineering, National University of Sciences & Technology, Islamabad, (Pakistan)

³Nanotechnologies Research Centre/Department of Physics, University of Engineering and Technology, Lahore, (Pakistan)

ABSTRACT

Variant concentrations of phenol formaldehyde resin were introduced into Acrylonitrile butadiene rubber (NBR) to investigate the high temperature ablation, thermal and mechanical properties of polymer-polymer composites. Ablation rates, percent char yields and insulation indexes were reduced, while the thermal conduction through the fabricated ablative composites was augmented with increasing phenolic resin blending concentration (PRBC) in the NBR matrix during the oxy-acetylene flame ablation test according to the ASTM E285-08. Thermal decomposition of the composite specimens was revealed thermal stability enhancement with increasing PRBC in the rubber matrix. Tensile strength and Shore A hardness of the ablators were progressed meanwhile the elongation at break suffered with increasing PRBC in the host matrix. Char morphology, polymer pyrolysis, char composition and polymer-polymer char interaction were analyzed using charred sample's photographs and scanning electron microscopy coupled with energy dispersive spectroscopy.

I. INTRODUCTION

A hypersonic and ultrahigh temperature environment is encountered by re-entry vehicles and solid rocket motors during their missions. Therefore to protect the space shuttle and rocket combustion chamber from the intense ablation atmosphere, ablative materials are used frequently. Polymer composites are widely used as ablative insulation materials in aerospace industry [1-3]. The selection of a suitable polymer and reinforcement is made on the basis of the hypothermal environment encountered by an aerodynamic body. An ablative composite insulates the incoming heat flux through the numerous heat absorbing, dissipating and reflecting mechanisms i.e. surface reradiation, polymer charring, transpirational, vaporization, char-reinforcement reactions, and reinforcement melting effects as elaborated in Fig. 1.

Two parameters have a key importance in ablation performance of an ablative material; first one is the ablation resistance and the second one is the thermal conduction through the ablator. Phenolic resin (Phenol Formaldehyde) based ablative composites have lower ablation/mechanical erosion rates but higher thermal conduction as compared to the elastomeric ablative composites based on nitrile butadiene rubber (NBR), ethylene propylene monomer rubber (EPDM), silicon rubber, etc [4-10]. An ideal condition for a better ablator

is high ablation resistance with low thermal conduction. NBR is an elastomeric material with low density, thermal conductivity and high heat capacity used to blend with phenol formaldehyde resin (PFR) with trade name Novalac [11].

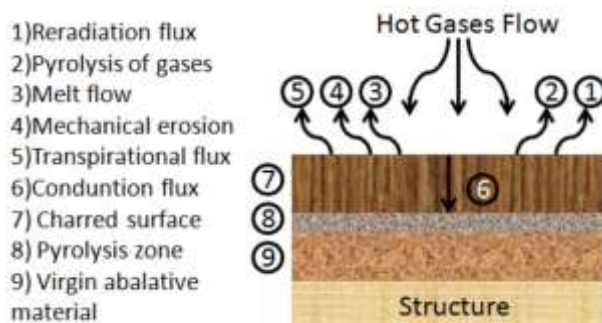


Figure 1. Schematic for Ablation Mechanism

Four progressive incorporations 0, 20, 25 and 30 wt.% of phenolic resin were incorporated into the rubber matrix were successfully made using two roller mixing mill and the fabricated ablative composites are named as NP1, NP2, NP3 and NP4, correspondingly. The main purpose of this polymer-polymer blending is to limit the ablation rates and thermal conduction through the NB–PFR (NBR/PR) ablative composites. Temperature sensing at the back-face of the NBR/PR composites was carried out using oxy – acetylene (O – A) torch flame for ablation testing according to the ASTM E285 – 08 [12]. Ablation resistance in head on impingement (HOI) and parallel flow (PF) modes of O–A flame was measured for the post burnt ablative specimens. Mechanical and thermal properties were evaluated to ensure the effect of PRBC on the thermo-mechanical properties of NP composites.

II. EXPERIMENTAL

2.1 Materials

Nitrile butadiene rubber (Kumho KNB 35L) was supplied by ABF International Corporation limited, Korea. Nanosilica, sulphur, zinc oxide and stearic acid were purchased from BDH. MBTS and TMTD were delivered by Dalian Richon Chemical Co. Ltd, China. DOP was purchased from International petrochemicals (Pvt) Ltd, Pakistan. PF resin (Novalac) was received from Plastics Engineering Company, Lakeshore Road, Sheboygan, U.S.A.

2.2 Fabrication of NP Composites

PF resin was blended with NBR using internal dispersion kneader and two roller mixing mill at specific temperature and rolling speed.. Sulphur was incorporated as a crosslinking entity; MBTS (Mercapto benzothiazole disulphide), and TMTD (Tetramethylthiuram disulfide) were used as accelerators; stearic acid and zinc oxide were utilized as activators; wax and DOP were used as plasticizers in the NBR matrix. Table I illustrates the composition scheme of the fabricated blended polymer composites. P& R ablators were fabricated on the hot isostatic press at 1600psi and 140°C for fifty minutes. P ablator had 100mm (L) * 100mm (W) * 10mm (T) dimensions for HOI ablation, while R ablator was similar to P ablator with a 10mm central cavity for PF ablation and tensile testing specimens were fabricated according to the ASTM D412–98A as depicted in Fig. 2.

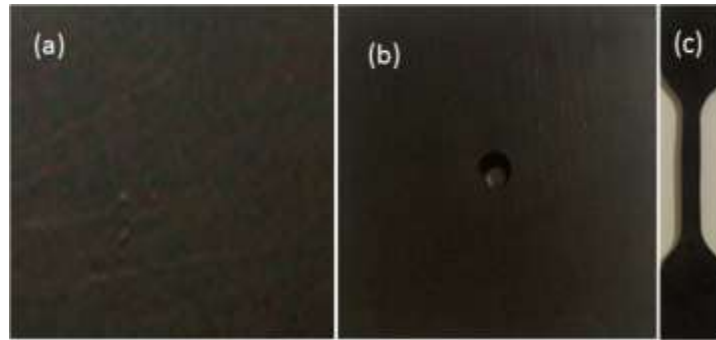


Figure 2. P (Linear ablative for head on impingement mode) and R (Radial ablative for parallel flow mode) ablators (a, b) and tensile sample (c) of NP composites

III. ABLATION TESTING

3.1 Backface Temperature Sensing

Fig. 3 illustrates the experimental setup ablation testing of NP composite specimens. A high temperature source (around 3000°C), O–A torch flame was kept 10mm far from the ablator's facet i.e. engraved in a domestically made ablative ceramic fixture.

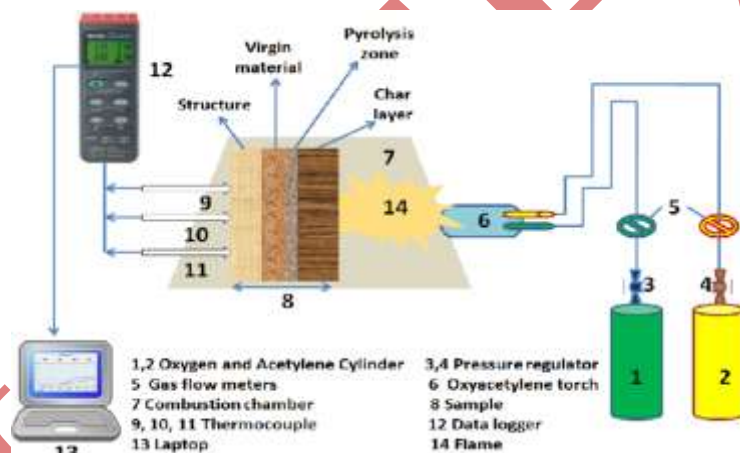


Figure 3. Schematic of Experimental Setup For Ablation Testing.

Oxygen and acetylene gases flow rates were 0.4l/m and 0.35L/m, respectively during the ablation testing. Back-face temperature at the P ablator's back facet was sensed with three special K–type thermocouples (–200–1350°C) i.e. connected with the TECPEL 319 data logger which was also linked with a laptop via RS–232 data cable. Meanwhile time–temperature contours for all thermocouples were established on the laptop screen using DTM 319 software. O–A torch was used in HOI and PF modes for P and R ablators, respectively to evaluate the ablation resistance and percent char yield in linear and radial directions, correspondingly.

3.2 Ablation Rates

Linear/mass ablation rates for P ablator, radial/mass ablation rates for R ablator and % char yield for both types were evaluated by using the following relations [13].

$$\text{Linear ablation rate of P ablator} = (\text{Initial thickness} - \text{Final thickness}) / \text{Ablation Time} \quad (1)$$

$$\text{Mass ablation rate of P ablator} = (\text{Initial mass} - \text{Final mass}) / \text{Ablation Time} \quad (2)$$

$$\text{Radial ablation rate of R ablator} = (\text{Initial diameter} - \text{Final diameter}) / \text{Ablation Time} \quad (3)$$

$$\text{Mass ablation rate of R ablator} = (\text{Initial mass} - \text{Final mass}) / \text{Ablation Time} \quad (4)$$

$$\% \text{ char yield for P ablator} = ((\text{Initial mass} - \text{Final mass}) * 100) / \text{Initial mass} \quad (5)$$

$$\% \text{ char yield for R ablator} = ((\text{Initial mass} - \text{Final mass}) * 100) / \text{Initial mass} \quad (6)$$

$$\text{Insulation Index (I}_T\text{)} = (\text{Time at temperature } ^\circ\text{C}) / \text{thickness} \quad (7)$$

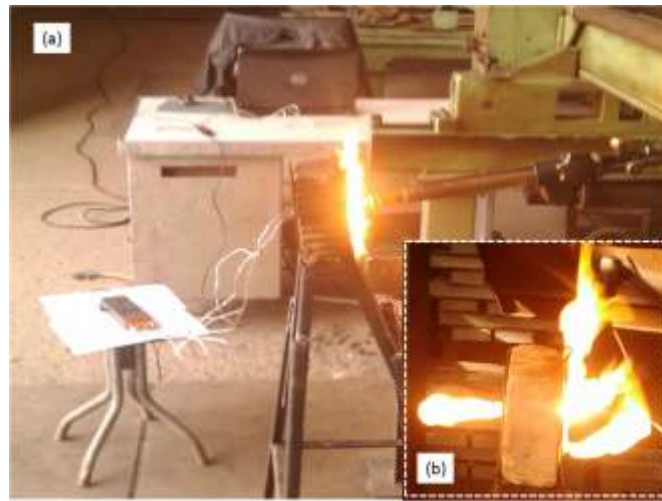


Figure 4. Online ablation testing in HOI mode (a) for P ablator and (b) PF mode for R ablator

A practical illustration of ablation testing in HOI and PF modes of O–A torch flame for P and R ablative composites at Pakistan Railway Carriage factory, Islamabad as elaborated in Fig. 4.

3.3 Thermogravimetric and Differential Thermal Analyses

TG/DTA was performed using Perkin Elmer Diamond TG/DTA apparatus to find out the thermal stability and endothermic/exothermic responses of the NP composites.

4. Mechanical Properties

Universal tensile machine (UTM, 20KNXD Plus, Shimadzu) was used to evaluate ultimate tensile strength, elongation at break and percent modulus of elasticity for the fabricated composites. Shore A hardness of the NP ablators were measured using rubber hardness tester (Torsee, Tokyo testing machine MFG.Co., Ltd.).

5. Spectroscopic Characterization

Scanning electron microscopy (SEM, JSM 6490A, Jeol, Japan) and energy dispersive spectroscopy (EDS) were performed to elaborate char morphology, char–reinforcement interaction, voids formation and composition of the post burnt NP ablative.

6. Results and Discussion

6.1 Back-Face Temperature Monitoring

Time–temperature contours were developed meanwhile on the laptop screen during the O–A flame exposure on the P ablator facet and they are depicted in Fig. 5. A typical NP composite, temperature profile describes the temperature evolution initially up to 50⁰C for the first 100 seconds exposure and in the second half thermal conduction through the ablator enhances but remains in limit due to the heat quenching phenomena take place within the ablator [14].

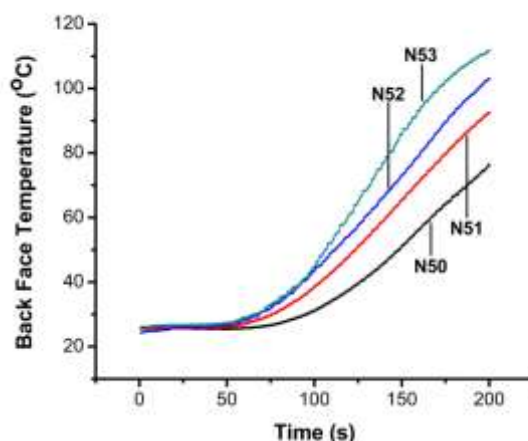


Figure 5. Back Face Time-Temperature Profile of NP Composites.

O–A flame temperature was around 3000°C and ablative front surface temperature was near about 1600°C as measured from the radiation pyrometer (IRAH 35U, Japan), NP1 ablative composite slows down the thermal conduction through the following mechanisms

- Transpirational cooling of volatile molecules of Dioctylephthalate (DOP)
- Water evaporation
- Heat reradiational effect
- Silica melting
- Char formation
- Polymer pyrolysis
- Char reinforcement reactions
- Hot gases exhaust

The peak back-face (BF) temperature ascending order is NP1<NP2<NP3<NP4, that shows that as the PFR wt.% increases in the NBR matrix, temperature evolution rate increases due to the excess conductive nature of PFR as compared to the elastomeric rubber, counterpart. The plus point of PFR is its high mechanical erosion and linear/radial ablation resistance in hypersonic and hyperthermal environments encountered by an aerodynamic surface. The peak BF temperature through the NP4 ablator is (110°C) i.e. less than the pristine PFR based ablators as reported in contemporary data which shows that NBR-PFR blending has a progressive impact regarding high temperature heat insulation [15]. Insulation indexes (I_T) at 50, 60, and 70°C of the NP ablators were measured according to the (Eq. 7) and are depicted in Table II. A descending order of I_T for NP1–NP4 is observed with increasing PRBC in the elastomeric rubber matrix which disclosed that NP4 can survive for longer period than the other ones in the hyperthermal environment.

6.2 Ablation Rates

Addition of phenolic resin to the NBR matrix efficiently decreases the ablation rates as depicted in Fig. 6. Ablation rates were measured according to the mathematical (Eqs. 1 and 4). Least linear/mass ablation rates were measured for NP4 ablator in HOI mode i.e. 0.011mm/sec and 0.15g/s, respectively as clear from Fig. 6a.

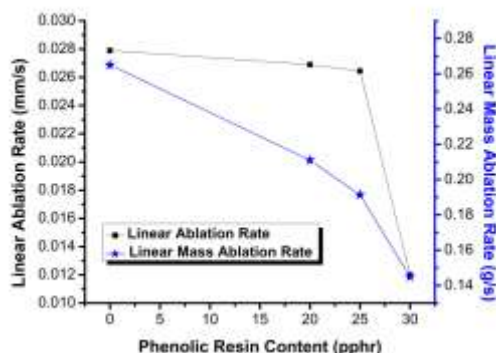


Figure 6a. Linear ablation rates of 'P' ablators

In PF mode of O–A flame through the 10mm cavity, minimum radial/mass ablation rates were observed for NP4 i.e. 0.14mm/s and 0.08g/s, respectively as depicted in Fig. 6b.

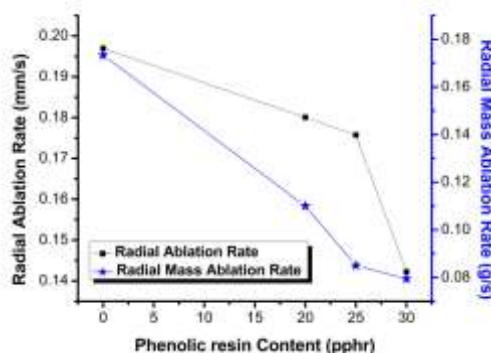


Figure 6b. Radial ablation rates of 'R' ablators

Ablation resistance descending order for all ablators is NP4> NP3>NP2>NP1. Percent char yield was also measured according to the (Eqs. 5 and 6). NP4 has least % char yield in both HOI and PF ablation modes for P and R ablators as clear from the Fig. 6c. Phenolic resin incorporation in the rubber matrix has improved the ablation resistance and reduced the percent char yield of the fabricated composites due to the PF resin uniform blending, organic compatibility with the host polymer matrix, high thermal stability and superb mechanical/ablation resistance of PFR as reported by Tea Jin K. et al [16].

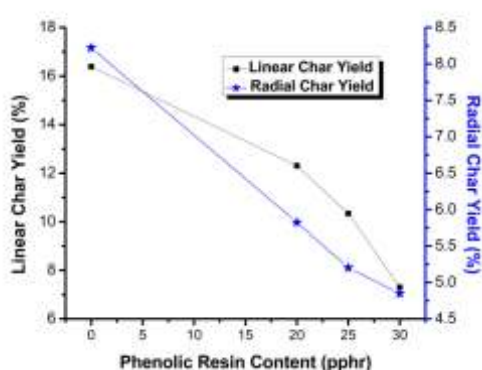


Figure 6c. Percent char yield for P & R ablators.

Post burnt ablated composites in HOI and PF modes are depicted in Post burnt P and R ablator are depicted in Fig. 7 and a strong interaction between ablative char and virgin polymer zone is observed which helped to minimize the ablative/mechanical recession against the hot stream of O–A flame gases [19].

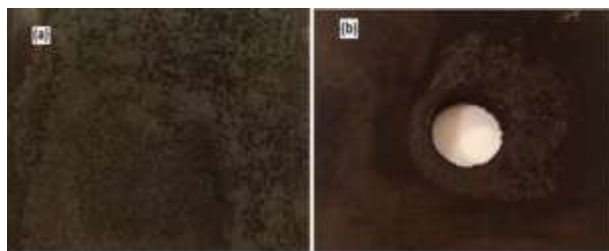


Figure 7. Photographs of charred P (a) & R (b) NP ablators

Polymer pyrolysis, voids formation, silica melting and composition of the NP4 ablator are illustrated in Fig. 8.

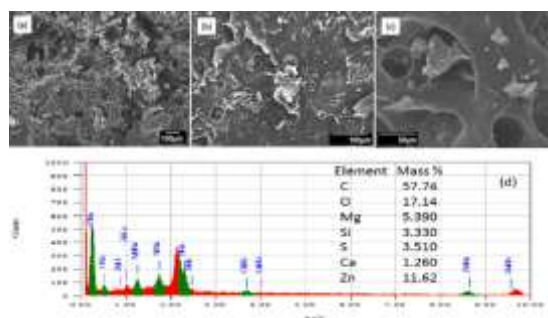


Figure 8. SEM micrographs, polymer pyrolysis (a); voids formation(b); silica melting(c) and compositional analysis(d) NP composites

These pores help to enhance the transpirational and vaporization cooling effects due to water, hot gases and organic oil evaporation [20-23].

6.3 Thermal Oxidation And Differential Thermal Analysis

Thermogravimetric and differential thermal analyses in the temperature range 25 to 800°C were performed and portrayed in Fig. 9a.

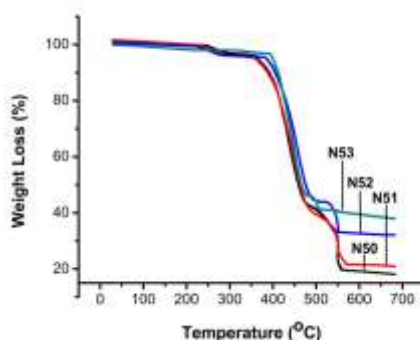


Figure 9a. Thermal Decomposition of NP Composites.

NP composites show thermal stability up to 300°C, and then deterioration is observed due to oil evaporation followed by a sudden steep due to polymer pyrolysis (300-550°C). Thermal gravimetric stability of NP composites is reduced as NP4>NP3>NP2>NP1 due to the increasing PRBC in the NBR matrix due to homogeneous polymer–polymer blending and high thermal degradation stability of PFR as compared to the elastomeric rubber [17]. NP4 has 44, 6, and 32% better thermal stability at 300, 500, and 650°C, respectively than the NP1 ablator as elaborated in Table III. DTA contours in Fig. 9b elaborate an exothermic response in temperature range 100-300°C due to oil evaporation and scoop out of hot gases and then an endothermic progress is observed due heat absorption through polymer pyrolysis [18]. NP4 has absorbed the maximum input heat due to maximum PRBC in the NBR matrix and polymer–polymer strong interaction.

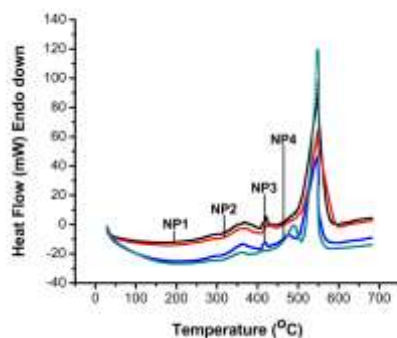


Figure 9b. Endo/Exothermic Behavior of NP Composites

6.4 Mechanical Properties

6.4.1 Ultimate Tensile Strength

Stress– strain contours, elongation at break, tensile strength, 50% and 100% modulus are elaborated in Fig. 10a and Table IV. Ultimate tensile strength, 50 and 100% modulus for NP composites are augmented while the elongation at break suffered as increasing PRBC in the rubber matrix which illustrated a tough to brittle behavior for NP1–NP4, gradually. Phenolic resin has a stiff thermosetting polymer that reduced the ductility and enhanced the stiffness of NP composites [21-23].

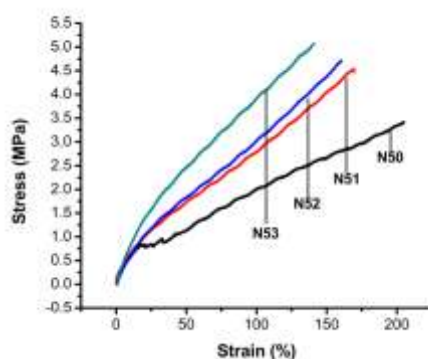


Figure 10a. Stress –Strain Curves of NP Composites

6.4.2 Hardness (Shore A:)

Shore A hardness trend is depicted in Fig. 10b which illustrated an augmentation with increasing PRBC in the NBR matrix due to the hard character of phenolic resin that was interacted with rubber polymeric chains and improved the NP composites hardness. Phenolic resin impregnation in the host elastomeric matrix effective enhanced the hardness level owing to the reduction in chain mobility/flow under pressure/force.

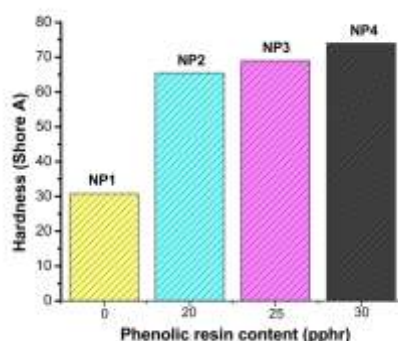


Figure 10b. Elastomeric hardness of NP composites

VII. CONCLUSION

A thermosetting resin, phenol formaldehyde is successfully blended with NBR matrix using internal dispersion kneader and two roller mixing mill. Ablation resistance of the NP composites was augmented meanwhile the thermal conduction through the ablator enhanced with increasing PRBC in the rubber matrix. Thermal stability of the fabricated composites was improved with increasing PRBC in the elastomeric polymer. Tough to brittle behavior with improved tensile strength is observed for the ablative composites with the addition of PRBC in the rubber matrix. Shore A hardness of the NP composites were also enhanced with the progressive phenolic resin insertion in the host matrix due to the hard segments of PF resin.

ACKNOWLEDGEMENT

The authors would like to greatly acknowledge that this work was completed with the cooperation of Longman Mills, Lahore and Pakistan Railway Carriage Factory, Islamabad.

REFERENCES

- [1] Wen, S. L. 2005. Steady ablation on the surface of a two-layer composite, *International Journal of Heat Mass Transfer*, **48**; 5504–5519,
- [2] Pulci, G., Tirillò, J., Marra, F., Fossati, F., Bartuli, C. and Valente, 2010. Carbon–phenolic ablative materials for re-entry space vehicles: Manufacturing and properties, *Composites: Part A*, **41**;1483–1490
- [3] Ahmad R.B., Mehrdad K., Navid M.H.F., and Beheshty M.H. 2006. Ablation and thermal degradation behaviour of a composite based on resol type phenolic resin: Process modeling and experimental, *Polymer*, **47**; 3661–3673
- [4] Jong K. P., Donghwan Cho., and Tae, J. K. 2004. A comparison of the interfacial, thermal, and ablative properties between spun and filament yarn type carbon fabric/phenolic composites, *Carbon*, **42**; 795–804
- [5] Jong K. P. and Tae J. K. 2002. Thermal and ablative properties of low temperature carbon fiber–phenol formaldehyde resin composites, *Carbon*, **40**; 2125–2134
- [6] Shuguo C., Haiyang Y., Wentan R. and Yong Z. 2009. Thermal degradation behavior of hydrogenated nitrile-butadiene rubber (HNBR)/clay nanocomposite and HNBR/clay/carbon nanotubes nanocomposites, *Thermochimica Acta*, **491**; 103–108
- [7] Zhang C., Kaushik P., Byeon J. U., Sang M. H. and Jin K. K. 2011. A Study on Mechanical and Thermal Properties of Silicone Rubber/EPDM Damping Materials, *Journal of Applied Polymer Science*, **119**; 2737–2741
- [8] Jun C., Wei W., Tingting Z. Wei F. and Qizhen L. 2011. Thermal Properties of the PA66/PC/ Silicone Rubber Composites, *Journal of Macromolecular Science Research .Part B: Physics*, **50**; 111–122
- [9] Donald R.P. and James E.M., 2010. Fillers for polysiloxane (“silicone”) elastomers, *Progress Polymer Science*, **35**; 893–901
- [10] Guoxin G., Zhicheng Z., Xuefei L., Qingjie M. and Yuansuo Zheng. 2010. An excellent ablative composite based on PBO reinforced EPDM, *Polymer Bulletin*. **64**; 607–622
- [11] Srebrenkoska V., Gordana B.G. and Dimko D. 2009. Composite material based on an ablative phenolic resin and carbon fibers, *Journal of Serbian Chemical Society*, **74** (4); 441–453

- [12] Tariq S.N., Amel M.N. and Mahmood M.B. 2008. Thermal and Ablative Properties of Ipnns and Composites of High Ortho Resole Resin and Difurfurylidene Acetone, *Leonardo Electronic Journal of Practices and Technologies*, **34**-46
- [13] Yue G., Ling-Xin Z., Li-Qun Z. and Yong-Lai L. 2011. Study on ablative properties and mechanisms of hydrogenated nitrile butadiene rubber (HNBR) composites containing different fillers, *Polymer Degradation Stability*, **96**; 808-817
- [14] Ahmad. R. B. and Mehrdad, K. 2009. Ablation mechanism of polymer layered silicate nanocomposite heat shield, *Journal of Hazardous Materials*, **166**; 445–454
- [15] Khan M.B, Nadeem. I, and Zaheer H., 2009. Transpiration Cooling Assisted Ablative Thermal Protection of Aerospace Substructures, *Key Engineering Materials*, **442**; 34-40
- [16] Tae J. K., Seung J. S., Kyunho J., and Jong K. P. 2004. Mechanical, thermal and ablative properties of interplay continuous/spun hybrid carbon composites, *Carbon*, **44**; 833–839
- [17] Bibin J., Dona M., Deependran B., George J., Reghunadhan C.P., Ninan K.N. 2011. Medium-density ablative composites: processing, characterization and thermal response under moderate atmospheric re-entry heating conditions, *Journal of Material Science*, **46**; 5017–5028
- [18] Maurizio N., Marco M., Debora P., José Maria K. and Luigi T. 2012. Ablative properties of carbon black and MWNT/phenolic composites: A comparative study, *Composites. Part A*, **43**; 174–182
- [19] Wang J. J., Feng L. J., Lei A. L., Yan A. J. and Wang X. J. 2012. Thermal Stability and Mechanical Properties of Room Temperature Vulcanized Silicone Rubbers, *Journal of Applied Polymer Science*, **125**; 505–511
- [20] Rajkumar, K., Nivashri, K., Ranjith, P., Chakraborty, S.K., 2011. Thavamani, P., Pazhanisamy, P. and Jeyanthi, P. High Temperature Resistance Properties of NBR Based Polymer Nanocomposites, *International journal of Chem Tech research*, **3(3)**; 1343-1348
- [21] Eung S.K., Tea H.L., Sung H.S., Jin-San Y. 2011. Effect of Incorporation of Carbon Fiber and Silicon Carbide Powder into Silicone Rubber on the Ablation and Mechanical Properties of the Silicone Rubber-Based Ablation Material, *Journal of Applied Polymer Science*, **120**; 831–838
- [22] Nadeem Iqbal, Sadia Sagar, Mohammad Bilal Khan, Hafiz Muhammad Rafique, 2013. Elastomeric ablative nanocomposites used in hyperthermal environments, *Polymer Engineering & Science*, **54**, 255-263
- [23] Sadia Sagar, Nadeem Iqbal, AsghariMaqsood, Umair Javaid, 2011. Thermogravimetric, differential scanning calorimetric and experimental thermal transport study of MWCNT/NBR nanocomposites, *Journal of Thermal Analysis and Calorimetry*, **114**, 161-167